



Pergamon

Available online at [www.sciencedirect.com](http://www.sciencedirect.com)

SCIENCE @ DIRECT®

Materials Research Bulletin 38 (2003) 1645–1651

Materials  
Research  
Bulletin

[www.elsevier.com/locate/matresbu](http://www.elsevier.com/locate/matresbu)

# Giant positive magnetoresistance in non-magnetic bismuth nanoparticles

Junwei Wang<sup>a</sup>, Guanghan Cao<sup>b</sup>, Yadong Li<sup>a,\*</sup>

<sup>a</sup>*Department of Chemistry and the Key Laboratory of Atomic & Molecular Nanosciences (Ministry of Education, China), Tsinghua University, Beijing 100084, PR China*

<sup>b</sup>*Department of Physics, Zhejiang University, Hangzhou 310027, PR China*

Received 24 January 2003; received in revised form 25 June 2003; accepted 2 July 2003

---

## Abstract

Large positive magnetoresistance of Bi nanoparticles, comparable with that in Bi thin film or nanowire arrays, has been shown here. Bi nanoparticles of average particle diameters of 50 or 100 nm were fabricated and giant magnetoresistance was observed near room temperature. In a field of 8 T, MR in 100 nm Bi nanoparticles, which is 230% at 10 K or 80% at 300 K, is larger than that in 50 nm Bi nanoparticles, which is 100% at 10 K or 40% at 300 K. The MR effect in bismuth may be related with its layer structure.

© 2003 Elsevier Ltd. All rights reserved.

*Keywords:* A. Metals; A. Nanostructures; B. Chemical synthesis; D. Magnetic properties; D. Electrical properties

---

## 1. Introduction

Giant magnetoresistance (GMR) effect has stimulated great interests of physicists and material scientists, due to its application in magnetic information storage, sensors and magnetoelectronics [1]. GMR was observed in many multilayers of ferromagnetic and nonmagnetic materials, as a consequence of the fact that the relative orientation of the magnetization of successive ferromagnetic layers changes from antiparallel to parallel in an applied field [2–4]. GMR also occurs in nonmultilayer granular solids, owing to spin-dependent scattering at the interfaces between the particles and the matrix [5,6]. Most reported GMR values, particularly those in spin-valve devices, are much smaller, in the range of 10% at room temperature. Certain suitable doped manganese perovskites, due to an insulator–metal transition, exhibit negative colossal magnetoresistance (CMR) [7,8]. However, the large effect size of CMR occurs

---

\* Corresponding author. Tel.: +86-10-62772350; fax: +86-10-62788765.  
E-mail address: [ydli@mail.tsinghua.edu.cn](mailto:ydli@mail.tsinghua.edu.cn) (Y. Li).

predominantly at low temperature and at room temperature the CMR effect is small. Moreover, the resistances of these perovskites are very large. This precludes most practical applications.

Recently, several nonmagnetic materials possessing GMR at room temperature were successfully exploited. The silver chalcogenides,  $\text{Ag}_2\text{Se}$  and  $\text{Ag}_2\text{Te}$ , are nonmagnetic materials, but their electrical resistance can be made very sensitive to magnetic field by slightly altering the stoichiometry [9–11]. It is interesting that the resistance of  $\text{Ag}_2\text{Se}$  exhibits an unusual linear dependence on magnetic field, based on which magnetic-field sensors are achieved [12]. Bismuth is a semimetal with highly anisotropic Fermi surface, high mobilities, long carrier mean free path and small effective carrier masses and thus provides an effective system to study quantum transport, large MR and finite-size effects. Chien group observed very large magnetoresistance in single-crystal bismuth thin films, which were fabricated by electrodeposition from aqueous solution of  $\text{Bi}(\text{NO}_3)_3 \cdot 5\text{H}_2\text{O}$  followed by suitable annealing, up to 300% at room temperature and 400,000% at low temperature in a field of 5 T [13,14]. MR of bismuth nanowire arrays was also studied, but the value in low magnetic field (up to 5 T) was small [15,16]. Herein, we show large positive magnetoresistance and finite-size effect in bismuth nanoparticles. MR of 100 nm Bi nanoparticles can reach up to 80% at room temperature and 230% at 10 K in a field of 8 T.

## 2. Experimental

Bismuth nanoparticles were prepared through a direct reduction from  $\text{Bi}(\text{NO}_3)_3 \cdot 5\text{H}_2\text{O}$  in the presence of  $\text{KBH}_4$  or  $\text{N}_2\text{H}_4 \cdot \text{H}_2\text{O}$ . In brief, for 50 nm bismuth nanoparticles, appropriate amount of bismuth nitrate was dissolved in Triton X-100 and then  $\text{KBH}_4$  was applied as reducing agents at room temperature. The solution was stirred strongly in the whole process. For 100 nm bismuth nanoparticles, some bismuth nitrate and aqueous hydrazine solution ( $\text{N}_2\text{H}_4 \cdot \text{H}_2\text{O}$ , 80% (v/v), 15 ml) were put into a Teflon-lined stainless steel autoclave with distilled water up to the 70% volume. The autoclave was sealed and maintained at 80 °C for 12 h. X-ray diffraction (XRD), scanning electron microscopy (SEM) and transmission electron microscopy (TEM) were used to characterize the products. The samples were ground and pressed into pellets under a pressure of 20 kg/cm<sup>2</sup> and without further annealed. Resistivity and MR were measured in a standard four-probe method in magnetic field up to 8 T.

## 3. Results and discussion

Fig. 1 shows the XRD pattern of as-synthesized 100 nm bismuth nanoparticles, which is similar with that of 50 nm bismuth nanoparticles. All of the reflections can be readily indexed to pure rhombohedral bismuth with lattice constants comparable with the values given in JCPDS 05-0519. TEM images in Fig. 2a and b reveal that these products are composed of nanoparticles with diameters of  $45 \pm 8$  nm or  $100 \pm 10$  nm, respectively. The surface of the pellets pressed from the powders was examined by SEM. Fig. 3 shows the SEM image of the pellet from 100 nm bismuth nanoparticles, indicating a fairly clean and smooth surface of the pellet.

The temperature-dependent resistivity of bismuth nanoparticles in zero field, 4 and 8 T is shown in Fig. 4. The resistivity is almost temperature independent at temperature less than 50 K, and above 50 K the resistivity decreases rapidly with increasing temperature, which shows Bi nanoparticles display a

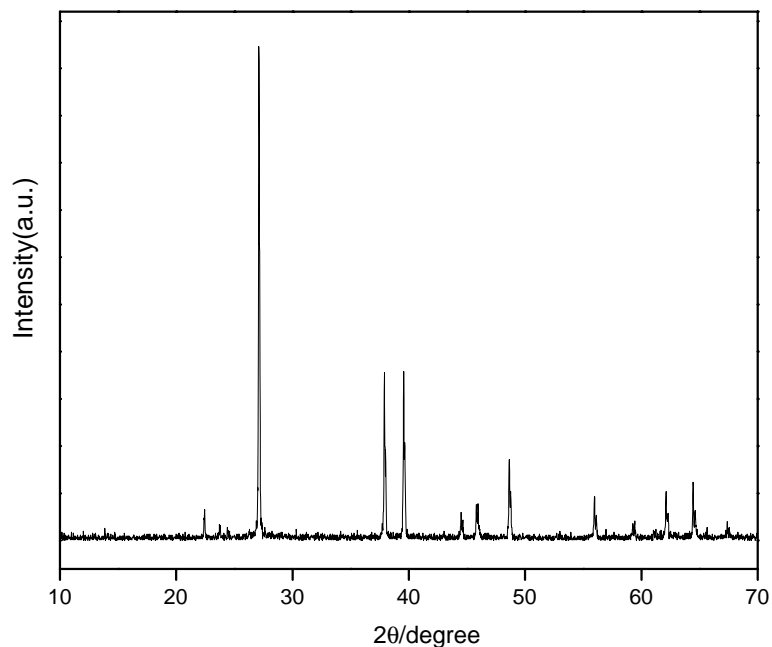


Fig. 1. XRD pattern of 100 nm Bi nanoparticles prepared in the presence of hydrazine. It is similar with that of 50 nm Bi nanoparticles synthesized in the presence of  $\text{KBH}_4$ .

semiconductor characteristic. The MR amplitude increases from about 80% at room temperature to more than 200% at 10 K. These values are much smaller than that in single crystalline Bi film observed by Chien group, due to electron scattering at the boundaries between the particles in our samples.

The resistance of the Bi nanoparticles at 10 and 300 K is shown in Fig. 5. Both the samples show quasilinear field dependence at low field up to 5 T. The field dependence of MR for Bi nanoparticles is shown in Figs. 6 and 7. For both 50 and 100 nm bismuth nanoparticles, the field dependence of MR is

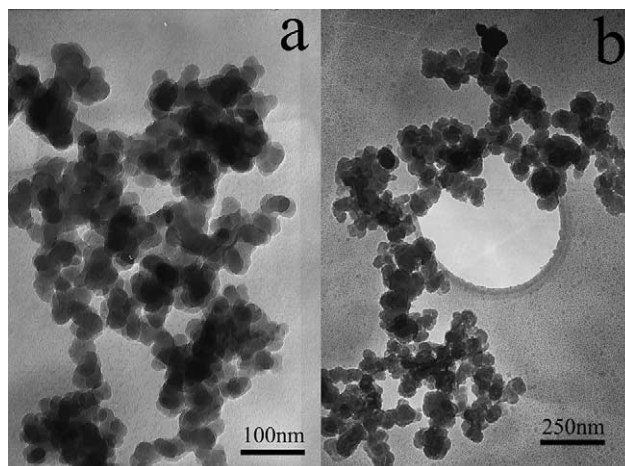


Fig. 2. TEM images of 50 and 100 nm bismuth nanoparticles.

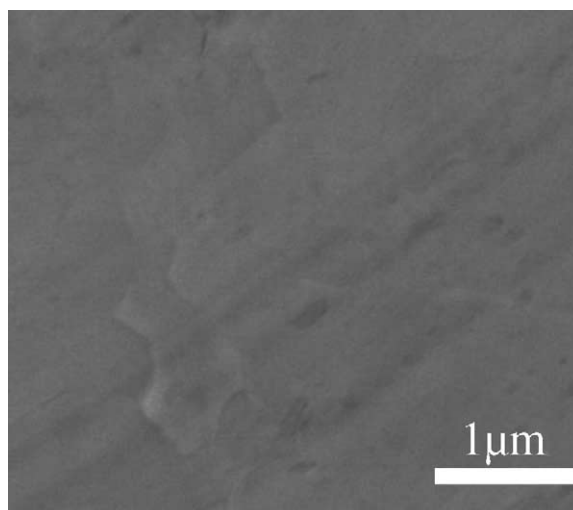


Fig. 3. SEM image of the pellet of 100 nm bismuth nanoparticles.

quasi-linear and does not saturate in the field range. As expected, the MR is symmetric with the field. The MR of Bi nanoparticles with average diameter 100 nm is larger (230, 80% at 10 and 300 K, respectively) than that of 50 nm diameter Bi nanoparticles (80, 40% at 10 and 300 K, respectively), showing a similar finite-size effect which was reported earlier [13,14,17,18]. The MR effect in Bi nanoparticles is the so-called ordinary MR, which arises from curved orbits in a magnetic field caused

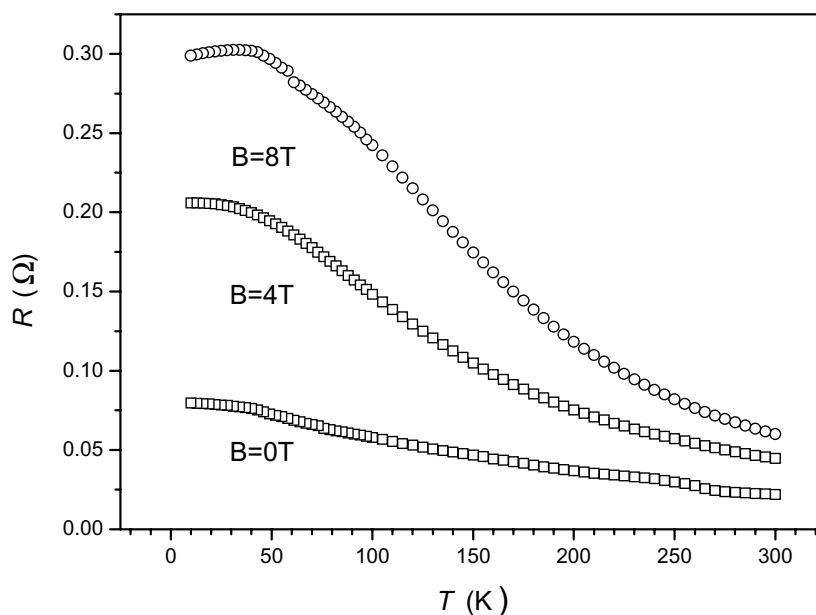


Fig. 4. Temperature dependence of resistivity of 100 nm bismuth with and without magnetic field.

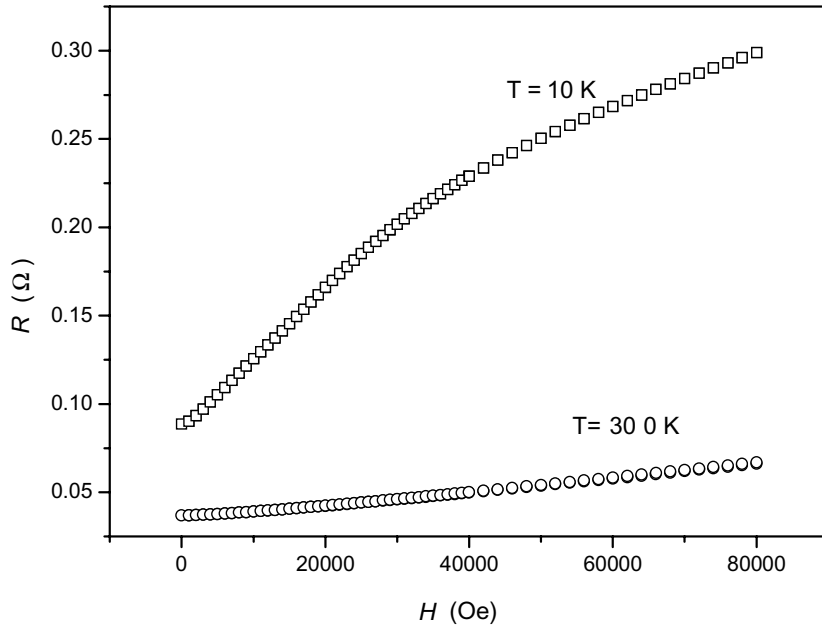


Fig. 5. Field dependence of resistivity of 100 nm bismuth at 10 and 300 K.

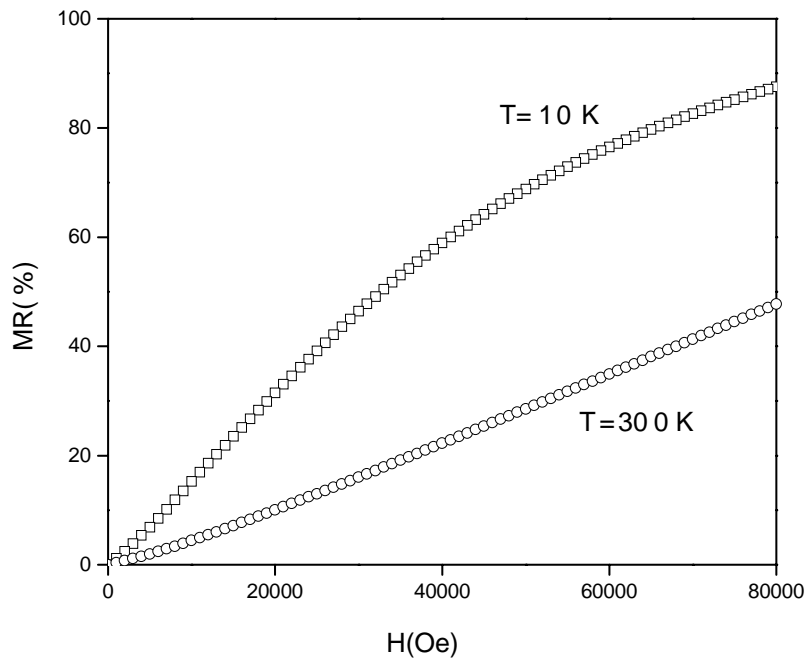


Fig. 6. Field dependence of magnetoresistance of 50 nm Bi nanoparticles at 10 and 300 K.

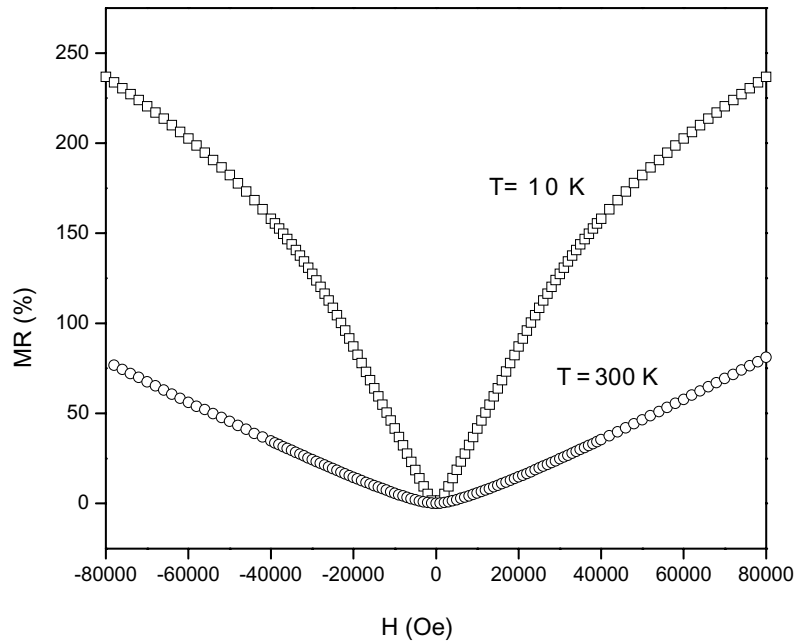


Fig. 7. Field dependence of magnetoresistance of 100 nm Bi nanoparticles at 10 and 300 K.

by Lorentz force. The ordinary MR is proportional to the product of the cyclotron frequency,  $\omega_c = eB/m \times c$ , and the relaxation time,  $\tau$ . In Bi,  $\omega_c$  is large because of the small nominal electron effective mass of  $0.002m_e$ . The relaxation time  $\tau$  is determined by the carrier mean-free-path  $l$ . In our samples,  $l$  in 100 nm bismuth nanoparticles is longer than that of 50 nm nanoparticles, so the MR is also larger. However, the MR values are much smaller than that observed in single crystalline Bi film. The size effect lowers the MR values owing to electron scattering at the grain-boundaries. For single crystalline bismuth film, grain-boundary scattering is eliminated and MR value is very large. The MR and quantum confinement effect in bismuth nanoparticles reported here is similar with that in polycrystalline bismuth films with small grain sizes. The MR value is large in bismuth films with big grain sizes.

As is mentioned before, many layered structures have GMR effects. Bismuth also has a pseudolayer structure [19]. In each layer, one Bi atom is connected with three other Bi atoms according to the 8-N rule and thus forms a trigonal pyramid. These pyramids further form a folded bismuth layer by vertex-sharing. GMR effect occurs in bismuth, as in many other layer-structures [11].

#### 4. Conclusion

We have studied the magnetoresistance of Bi nanoparticles with different average diameters. The MR characteristic of bismuth nanoparticles is similar with bismuth films or nanowire arrays, however, the values vary with different sizes. Both the resistivity at zero field and MR show a strong dependence on the nanoparticles diameter because of the finite-size effect in these materials.

## Acknowledgements

This work was supported by the NSFC (20025102, 50028201, 20151001), the Foundation for the Author of National Excellent Doctoral Dissertation of P.R. China, and the State Key Project of Fundamental Research for nanomaterials and nanostructures.

## References

- [1] G.A. Prinz, *Science* 282 (1998) 1660.
- [2] M.N. Baibich, J.M. Broto, A. Fert, F. Nguyen van Dau, F. Petroff, P. Etienne, G. Creuzet, A. Friederich, J. Chazeles, *Phys. Rev. Lett.* 61 (1998) 2472.
- [3] S.S.P. Parkin, R. Bhadra, K.P. Roche, *Phys. Rev. Lett.* 66 (1991) 2152.
- [4] F. Petroff, A. Barthelemy, D.H. Mosca, D.K. Lottis, A. Fert, P.A. Schroeder, W.P. Pratt Jr., R. Loloee, S. Lequien, *Phys. Rev. B* 44 (1991) 5355.
- [5] A.E. Berkowitz, J.R. Mitchell, M.J. Carey, A.P. Young, S. Zhang, F.E. Spada, F.T. Parker, A. Hutten, G. Thomas, *Phys. Rev. Lett.* 68 (1992) 3745.
- [6] J.Q. Xiao, J.S. Jiang, C.L. Chien, *Phys. Rev. Lett.* 68 (1992) 3749.
- [7] R. von Helmolt, J. Wecker, B. Holzapfel, L. Schultz, K. Samwer, *Phys. Rev. Lett.* 71 (1993) 2331.
- [8] S. Jin, T.H. Tiefel, M. McCormack, R.A. Fastnacht, R. Ramesh, L.H. Chen, *Science* 264 (1994) 413.
- [9] R. Xu, A. Husmann, T.F. Rosenbaum, M.-L. Saboungi, J.E. Enderby, P.B. Littlewood, *Nature* 390 (1997) 57.
- [10] H.S. Schnyders, M.-L. Saboungi, T.F. Rosenbaum, *Appl. Phys. Lett.* 76 (2000) 1710.
- [11] I.S. Chuprakov, K.H. Dahmen, *Appl. Phys. Lett.* 72 (1998) 2165.
- [12] A. Husmann, J.B. Betts, G.S. Boebinger, A. Migliori, T.F. Rosenbaum, M.-L. Saboungi, *Nature* 417 (2002) 421.
- [13] F.Y. Yang, K. Liu, K. Hong, D.H. Reich, P.C. Searson, C.L. Chien, *Science* 284 (1999) 1335.
- [14] F.Y. Yang, K. Liu, C.L. Chien, P.C. Searson, *Phys. Rev. Lett.* 82 (1999) 3328.
- [15] J. Heremans, C.M. Thrush, Z. Zhang, X. Sun, M.S. Dresselhaus, J.Y. Ying, D.T. Morelli, *Phys. Rev. B* 58 (1998) R10091.
- [16] K. Hong, F.Y. Yang, K. Liu, D.H. Reich, P.C. Searson, C.L. Chien, F.F. Balakirev, G.S. Boebinger, *J. Appl. Phys.* 85 (1999) 6184.
- [17] F.Y. Yang, G.J. Strijkers, K. Hong, D.H. Reich, P.C. Searson, C.L. Chien, *J. Appl. Phys.* 89 (2001) 7206.
- [18] C.L. Chien, F.Y. Yang, K. Liu, D.H. Reich, P.C. Searson, *J. Appl. Phys.* 87 (2000) 4659.
- [19] R.W.G. Wyckoff, *Crystal Structures*, 2nd ed., vol. 1, Interscience, New York, 1973, p. 32.